Environmental Science and Ecotechnology 30 (2026) 100678

Contents lists available at ScienceDirect

Environmental Science and Ecotechnology

journal homepage: www.journals.elsevier.com/environmental-science-and-ecotechnology/

Original Research

Rhizosphere accelerates breakdown of large biodegradable microplastics in soil

Kailin Gong [a], Cheng Peng [a,b,*], Xiaoyi Chen [a], Li Cai [b,c], Wei Zhang [a]

[a] Key Laboratory of Environmental Risk Assessment and Control on Chemical Process, Ministry of Ecology and Environment, School of Resource and Environmental Engineering, East China University of Science and Technology, Shanghai, 200237, China
[b] Shanghai Institute of Pollution Control and Ecological Security, Shanghai, 200092, China
[c] College of Environmental Science and Engineering, Donghua University, Shanghai, 201620, China

ARTICLE INFO

Article history:
Received 27 June 2025
Received in revised form
16 February 2026
Accepted 22 February 2026

Keywords:
Biodegradable microplastics
Rhizosphere effect
Degradation
Microbial community
Soil metabolomics

ABSTRACT

The expanding deployment of biodegradable mulch films in global agriculture aims to mitigate persistent plastic pollution, yet the fate of resulting biodegradable microplastics (BMPs) in soil ecosystems remains poorly characterized. Although these materials are engineered for mineralization, their breakdown rates under realistic field conditions vary substantially, and plant roots fundamentally alter soil biogeochemistry through rhizodeposition and microbial recruitment. Whether the biochemically complex rhizosphere environment accelerates or retards BMP degradation, and how degradation byproducts accumulate, represents a critical knowledge gap for assessing the environmental safety of biodegradable agricultural plastics. Here we show that the soybean rhizosphere exhibits size-selective effects on poly(butylene adipate-co-terephthalate) microplastic (PBAT–MP) degradation. Large particles (998.7 ± 74.6 μm) degrade significantly faster than in bulk soil, whereas small particles (145.6 ± 3.1 μm) remain largely protected within soil aggregates over a 70-day growth cycle. Advanced quantitative proton nuclear magnetic resonance analysis reveals preferential hydrolysis of aliphatic adipate units, resulting in greater accumulation of degradation monomers in the rhizosphere than in bulk soil. Microbial community profiling identifies enrichment of Proteobacteria—particularly *Bradyrhizobium* and *Ramlibacter* genera—linked to PBAT hydrolysis and metabolite utilization, alongside increased microbial biomass and altered soil carbon pools. These findings challenge the prevailing assumption that biodegradable mulches degrade uniformly and benignly under agricultural conditions. Rhizosphere-relevant assessment criteria are essential for evaluating the true environmental safety of biodegradable plastics in agricultural systems, with broader implications for sustainable soil management and plastic pollution mitigation strategies worldwide.

1. Introduction

The widespread agricultural use of conventional plastics, particularly low-density polyethylene mulch films, has led to persistent macroplastic and microplastic (MP) contamination of soils [1]. Biodegradable mulch films, primarily composed of polymers such as poly(butylene adipate-co-terephthalate) (PBAT), have emerged as eco-friendly alternatives for reducing long-term plastic accumulation in global agroecosystems [2,3]. However, incomplete degradation of these films generates biodegradable microplastics (BMPs), raising concerns about their ecological impacts on agroecosystems [4]. Previous studies have quantified BMP mineralization rates under varying soil conditions (e.g., temperature, moisture, and nutrient availability) [5,6], but a critical knowledge gap persists regarding the role of plant roots in modulating BMP degradation.

Plant roots fundamentally shape soil biogeochemistry through rhizodeposition and selective microbial recruitment [7–9]. The rhizosphere environment is characterized by high carbon availability, nutrient limitations, and acidic conditions—factors that

* Corresponding author. Key Laboratory of Environmental Risk Assessment and Control on Chemical Process, Ministry of Ecology and Environment, School of Resource and Environmental Engineering, East China University of Science and Technology, Shanghai, 200237, China.
E-mail address: cpeng@ecust.edu.cn (C. Peng).

https://doi.org/10.1016/j.ese.2026.100678

can either enhance or inhibit BMP degradation [5,10,11]. The microbial community structure plays a pivotal role. Both the rhizosphere and plastisphere (the unique ecological niche created by MPs in soil [12]) favor copiotrophic bacteria [13,14], suggesting potential synergistic interactions. However, recent findings indicate that plant roots may disrupt plastisphere assembly processes [8]. Although BMPs have been shown to increase populations of potential degradative bacteria in the rhizosphere [4,15,16], the extent of this niche specialization, particularly compared with bulk soil microbial communities, remains to be investigated [17]. These uncertainties highlight the need to clarify how roots regulate BMP degradation relative to bulk soil.

Plants can accelerate the microbial degradation of synthetic polymers in soil [18,19]. However, studies have primarily relied on indirect measurements, such as weight loss, changes in mechanical properties, and surface modifications, without determining whether the lost polymer mass mineralizes completely or persists as MPs and nanoplastics (NPs). Isotope tracing provides more precise estimates of mineralization [2,20], while quantitative proton nuclear magnetic resonance (q-^{1}H NMR) enables direct measurement of biodegradable plastics in soil [21]. Applying these advanced techniques to investigate the influence of root systems on BMP degradation provides critical insights into rhizosphere-mediated polymer transformation processes.

In this study, we hypothesized that roots accelerate BMP degradation, and this effect is influenced by particle size. PBAT microplastics (PBAT–MPs) were selected as representative BMPs because PBAT is among the most widely produced biodegradable plastics and a primary component of biodegradable mulch films [22]. Soybean (*Glycine* max (L.) Merr.) was chosen due to its extensive global cultivation as a major food crop and its pronounced rhizosphere effects [7].

We employed the q-^{1}H NMR technique to quantitatively evaluate differences in the degradation rates of PBAT–MPs tested at two particle sizes (median diameters of 998.7 $\pm$ 74.6 μm and 145.6 $\pm$ 3.1 μm) and two concentrations (0.1% and 1% w/w) between the rhizosphere and bulk soil. We then quantified degradation products and characterized morphological and chemical changes in PBAT–MPs. To elucidate the mechanisms driving rhizosphere-enhanced biodegradation, we further analyzed soil physicochemical properties, microbial biomass, enzyme activities, bacterial community composition, and soil metabolic profiles.

2. Materials and methods

2.1. Chemicals

Chloroform ($CHCl_3$, high performance liquid chromatography (HPLC) grade) and methanol (MeOH, HPLC grade) were purchased from Sinopharm Chemical Reagent Co., Ltd. Deuterated chloroform ($CDCl_3$, 99.8 atom% D) and *p*-nitrophenyl butyrate (*p*NP-B, >99% purity) were obtained from Adamas-beta. 1,4-Dimethoxybenzene (DMB, >99% purity) and *p*-nitrophenol (*p*NP, >99% purity) were sourced from Macklin Biochemical Co., Ltd. All additional reagents for soil physicochemical analysis (purity >99%) were supplied by Sinopharm Chemical Reagent Co., Ltd.

2.2. BMPs and soil

This study used two PBAT–MP sizes (Supplementary Fig. S1), representing typical PBAT farmland residue sizes [23]. The detailed preparation protocol is described in Supplementary Text S1.

The bulk soil was collected from the top 20 cm of a Shanghai soybean field (30°57′ N, 121°03′ E) with no history of biodegradable plastic film use. The soil preparation methodology is detailed in Supplementary Text S2, and its physicochemical properties are presented in Supplementary Table S1. Flotation analysis detected approximately 367 MP items per kilogram in the original soil, with no detectable BMPs (Supplementary Fig. S2).

2.3. Soybean cultivation

The experimental design of this study is shown in Supplementary Fig. S3. The cultivation experiment was conducted in polypropylene pots containing 2 kg of soil mixed with PBAT–MPs at 0.1% w/w (environmentally relevant) and 1% w/w (anticipating increased use and uneven distribution) [23]. A 300-mesh (53 μm pore size) stainless steel barrier divided soybean roots (rhizosphere soil) from the bulk soil while permitting nutrient and water exchange in each pot (Supplementary Fig. S4).

Five treatments were established: BLK (no PBAT–MPs), L0.1 (0.1% large PBAT–MPs), L1 (1% large PBAT–MPs), S0.1 (0.1% small PBAT–MPs), and S1 (1% small PBAT–MPs), with each treatment replicated in triplicate. Surface-sterilized soybean seedlings were grown under natural conditions (15–39 °C, 42–97% relative humidity) for an entire life-cycle study (70 days), with soil moisture maintained at 60% maximum water-holding capacity (MWHC).

Plant growth indicators (Supplementary Fig. S5–S7) were measured at the flowering (Day 28), podding (Day 46), and filling stages (Day 63). After harvest at the mature stage of soybean growth, soil samples were collected from the outside (bulk soil) and inside (rhizosphere soil) of the steel mesh. Meanwhile, the plant biomass was measured (Supplementary Fig. S7). Detailed cultivation procedures are described in Supplementary Text S3.

The bulk soil samples were labeled B_BLK, B_L0.1, B_L1, B_S0.1, and B_S1; the rhizosphere samples were labeled R_BLK, R_L0.1, R_L1, R_S0.1, and R_S1. As soybean roots fully occupied the mesh-enclosed space, we designated the soil within the metal mesh as rhizosphere soil.

2.4. Quantification of PBAT–MPs and degradation products in soil

We used Nelson et al.'s [21] modified method to quantify PBAT–MPs in freeze-dried soil samples, combining ultrasonic extraction with q-^{1}H NMR spectroscopy detection. Specifically, PBAT–MPs were extracted with 90:10 (v/v) $CHCl_3$/MeOH under ice-bath sonication. The extracts were evaporated naturally in glass amber vials before being reconstituted in $CDCl_3$ containing known DMB amounts and transferred to an NMR tube for analysis. Detailed methods are presented in Supplementary Text S4.

The q-^{1}H NMR results showed linear responses for both sizes of PBAT–MPs in $CDCl_3$, with slopes of 0.99 and 1.00, respectively (Supplementary Fig. S8). The ^{1}H NMR spectra of the soil extracts exhibited minimal baseline noise, with well-resolved peaks suitable for integration analysis (Supplementary Fig. S9). Recovery rates for added PBAT–MPs were 99.1 $\pm$ 1.8% (large) and 97.2 $\pm$ 2.1% (small) (Supplementary Table S2).

PBAT degradation products—terephthalic acid (TPA), adipic acid (AA), and 1,4-butanediol—were extracted and quantified from soil samples following Hua et al.'s methodology [24]. The detailed procedure for monomer analysis is described in Supplementary Text S5.

2.5. Extraction and characterization of PBAT–MPs

We extracted PBAT–MPs from freeze-dried soil samples (L1 and S1 treatments) using an improved method based on Li et al. [25]. PBAT–MP morphology was identified using scanning electron microscopy (SEM; GeminiSEM 300, ZEISS, Oberkochen, Germany). Surface chemical composition was analyzed using attenuated total

reflection Fourier Transform Infrared spectroscopy (ATR–FTIR; Nicolet 6700, Thermo Fisher Scientific, Waltham, MA, USA) and Raman spectroscopy with a 785 nm laser (LabRAM HR Evolution, HORIBA Jobin Yvon, Longjumeau, France). The sample composition was measured using NMR (ASCEND 400 MHz NMR, Bruker, Billerica, MA, USA) with $CDCl_3$. We performed thermogravimetric analysis (TGA) using a thermogravimetric analyzer (TGA 3, Mettler Toledo, Greifensee, Switzerland). Thermal analyses were performed using differential scanning calorimetry (DSC; DSC 8500, PerkinElmer, Waltham, MA, USA). Detailed PBAT–MP extraction and characterization procedures are presented in Supplementary Text S6.

2.6. Analysis of soil water-stable aggregates

Air-dried soil samples were fractionated into four size classes of water-stable aggregates via wet sieving: >2000 μm (mega-aggregates), 250–2000 μm (macroaggregates), 53–250 μm (microaggregates), and <53 μm (silt and clay fractions) [26]. The detailed methodology is described in Supplementary Text S7.

2.7. Analysis of the physicochemical properties of soil

We used fresh soil samples at 60% MWHC to measure microbial biomass carbon (MBC) using the chloroform fumigation-extraction method [27]. Freeze-dried samples were used for pH (soil:water, 1:2.5) [28], dissolved organic carbon (DOC; soil:ultrapure water from a Milli-Q system, 1:10; shaken for 12 h) [29], total dissolved nitrogen (TDN; 2M KCl; soil:water, 1:2.5; shaken for 1 h) [30], nitrate nitrogen (NO_3^--N), ammonium nitrogen (NH_4^+-N), and dissolved organic nitrogen (DON; calculated as TDN minus NO_3^--N and NH_4^+-N) analysis. We quantified DOC and TDN using a total organic carbon analyzer (TOC-L, Shimadzu, Kyoto, Japan), and measured NO_3^--N and NH_4^+-N with a discrete analyzer (AQ300, SEAL Analytical, Mequon, WI, USA). Detailed procedures are provided in Supplementary Text S8.

We collected excitation-emission matrix (EEM) fluorescence spectra of dissolved organic matter (DOM) using a fluorescence spectrophotometer (F-7000, Hitachi High-Tech, Tokyo, Japan). Test parameters and data analysis details are presented in Supplementary Text S9.

2.8. Determination of esterase activity of soil and PBAT–MPs

We measured soil and PBAT–MP esterase activities using a modified method based on Tsuboi et al. [31], which employs *p*NP-B as a substrate and quantifies the *p*NP produced by esterase-mediated hydrolysis. For soil esterase activity, we analyzed fresh soil samples at 60% MWHC. For PBAT–MP-associated esterase activity, we isolated PBAT–MP particles from the rhizosphere and the bulk soil of the L1 group by wet sieving, with 28 particles per pot (14 from each zone). These particles were washed with phosphate-buffered saline buffer and placed in a 96-well plate for analysis. Detailed methods are provided in Supplementary Text S10.

2.9. 16S rRNA gene amplicon sequencing

We subjected bulk and rhizosphere soil samples from the BLK, L1, and S1 treatments to 16S rRNA gene amplicon sequencing. DNA was extracted from 0.50 g of soil (stored at −80 °C) using the E.Z.N.A. Stool DNA Kit (Omega Bio-Tek, Norcross, GA, USA), following the manufacturer's instructions. The partial 16S rRNA gene was amplified with a barcode-containing primer set 338F/806R and sequenced on a Sequel IIe System (Pacific Biosciences, Menlo Park, CA, USA). Detailed DNA extraction and sequencing methods are provided in Supplementary Text S11.

2.10. Determination of soil metabolism

We analyzed bulk and rhizosphere soil samples from the BLK, L1, and S1 treatments for soil metabolism. The samples were placed in 2 mL centrifuge tubes and stored at −80 °C. Metabolites were then extracted and analyzed using a UHPLC-Q Exactive HF-X system (Thermo Fisher Scientific, Waltham, MA, USA). Details on the extraction and instrument conditions are shown in Supplementary Text S12.

2.11. Data analysis

We assessed normality and homogeneity of variance using the Shapiro–Wilk and Levene tests before proceeding with further statistical analysis. Parameters tested included soybean growth and yield parameters, water-stable aggregates, soil physicochemical properties, PBAT–MP and degradation product content, esterase activity, fluorescent index (FI), biological index (BIX), and humification index (HIX).

A one-way ANOVA and a Tukey's post-hoc test were used to compare treatments (BLK, L0.1, L1, S0.1, and S1) when assumptions were met; otherwise, the Kruskal–Wallis test with Dunn's post-hoc test was applied. Within each treatment, we compared bulk versus rhizosphere soil using a two-sample *t*-test when assumptions were met; otherwise, we used the Mann–Whitney *U* test.

We also used a *t*-test to assess differences in the abundance-based coverage estimator (ACE), Shannon indices, and bacterial phylum abundances between treatments. Nonmetric multidimensional scaling (NMDS) based on Bray–Curtis distances for amplicon sequence variants (ASVs) was performed to evaluate bacterial community clustering. Bacterial co-occurrence networks based on Spearman correlation analysis were visualized in Gephi (v. 0.1).

We tested associations between soil physicochemical properties and bacterial communities using a Mantel test implemented in the R package vegan. We used partial least squares discriminant analysis (PLS–DA) to identify differential metabolites. Co-occurrence networks linking PBAT–MP degradation rates, bacterial families, and soil metabolites were visualized in Cytoscape (v. 3.9.1). Unless stated otherwise, we performed statistical analyses and generated plots in R (v. 4.3.3) and finalized figures in Adobe Illustrator 2022.

3. Results and discussion

3.1. PBAT–MP degradation and characterization in the soybean rhizosphere

After 70 days of incubation, the average degradation rates of PBAT–MPs in the bulk soil were relatively low, ranging from 1.4% to 3.7% (Fig. 1a and b). These rates are substantially lower than the 8–13% degradation after 40 days reported by Zumstein et al. [2] for PBAT films using ^{13}C-labeled polymers and isotope-specific analytical techniques. Compared to our experimental setup, the divergent experimental conditions set by Zumstein et al. [2]—neutral pH (7.5), 47% MWHC, and a constant 25 °C temperature—may have created more favorable degradation conditions.

Soybean roots significantly promoted PBAT–MP degradation in the L1 group ($p < 0.05$), where rhizosphere soil contained 0.92 ± 0.02% (w/w) compared to 0.96 ± 0.02% (w/w) in the bulk soil (Fig. 1a). This aligns with prior work on polylactic acid/PBAT blends, where larger particles (0.5–2.0 mm) degraded significantly (15.4% after 230 days) in dry soil, while smaller particles

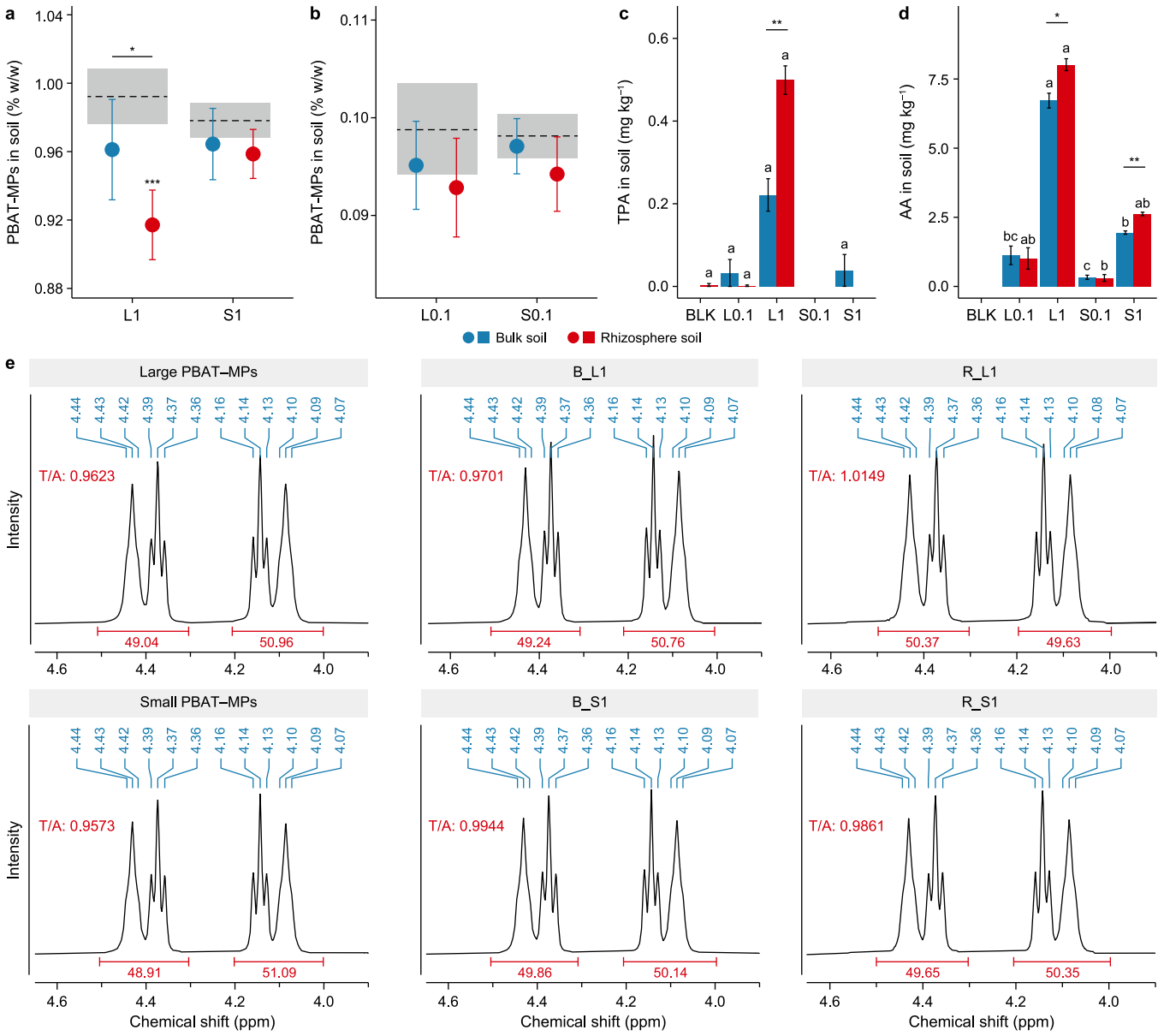

Fig. 1. Rhizosphere effects on poly(butylene adipate-co-terephthalate) microplastic (PBAT–MP) degradation and monomer release after soybean cultivation. **a**–**b**, Residual PBAT–MPs in bulk and rhizosphere soil at 0.1% (**a**) and 1% (**b**) PBAT–MP loading. Treatment: L0.1, 0.1% large PBAT–MPs; L1, 1% large PBAT–MPs; S0.1, 0.1% small PBAT–MPs; S1, 1% small PBAT–MPs. Dashed lines indicate pre-cultivation levels. Data are means ± standard deviation (SD) ($n = 6$). **c**–**d**, Terephthalic acid (TPA; **c**) and adipic acid (AA; **d**) concentrations in bulk and rhizosphere soil. Treatment: BLK, no PBAT–MPs. Lowercase letters indicate differences among treatments ($p < 0.05$). Data are means ± SD ($n = 3$). Asterisks indicate significant differences (*$p < 0.05$; **$p < 0.01$; ***$p < 0.001$). **e**, ^{1}H NMR spectra of extracted PBAT–MPs showing terephthalate-to-adipate (T/A) ratios. B_L1 and B_S1: bulk soil samples of L1 and S1 treatments; R_L1 and R_S1: rhizosphere samples of L1 and S1 treatments. Blue numbers indicate chemical shifts (ppm), while red intervals and values represent normalized peak areas.

(<0.5 mm) showed no significant degradation under both dry and wet conditions [6]. Similarly, mineralization studies of starch-blended PBAT–MPs across sizes (<100, 100–250, 250–500, 500–1000, 1000–2000, and 2000–4750 μm) showed size-dependent rates in Ferralsol (faster for smaller sizes except the largest) but minimal impact in Vertisol [5].

Concurrent with the degradation of PBAT–MPs, the monomers TPA and AA were detected in the soil, whereas 1,4-butanediol was not detected (Fig. 1c and d). This differential accumulation can be attributed to the distinct biodegradation kinetics of the three monomers. While 1,4-butanediol is ultimately mineralizable despite slower dissolution, TPA exhibits a pronounced lag phase and incomplete degradation, and AA degrades relatively slowly, enabling transient accumulation [32].

TPA was predominantly detected in the L1 treatment, with concentrations in the rhizosphere soil (0.50 ± 0.06 mg kg^{-1}) exceeding those in the bulk soil (0.22 ± 0.07 mg kg^{-1}) by 125.5% ($p < 0.01$; Fig. 1c). AA occurred in all PBAT–MP treatments, following a size-dependent trend. In the bulk soil, AA concentrations decreased in the order L1 (6.72 ± 0.46 mg kg^{-1}), S1 (1.95 ± 0.10 mg kg^{-1}), L0.1 (1.12 ± 0.58 mg kg^{-1}), and S0.1 (0.33 ± 0.13 mg kg^{-1}). In rhizosphere soil, AA concentrations decreased in the following order: L1 (8.02 ± 0.37 mg kg^{-1}), S1 (2.62 ± 0.11 mg kg^{-1}), L0.1 (1.01 ± 0.67 mg kg^{-1}), and S0.1 (0.31 ± 0.21 mg kg^{-1}). Notably, AA concentrations in the rhizosphere soil were significantly higher than in the bulk soil by 19.3%

and 34.5% in the L1 and S1 treatments, respectively ($p < 0.05$; Fig. 1d).

The elevated TPA and AA levels in the L1 rhizosphere soil correlated with the significant PBAT–MP degradation observed in this treatment (Fig. 1a). Furthermore, the greater accumulation of AA compared to TPA (Fig. 1c and d) indicates the preferential degradation of aliphatic adipate units over aromatic terephthalate units within the PBAT polymer [2]. The accumulation of these degradation byproducts, especially the aromatic monomer TPA, raises ecotoxicological concerns, as TPA is a known biotoxin that can persist in soil at hazardous concentrations (131 mg kg^{-1}) [33,34]. Moreover, AA was detected at higher concentrations in the L1 treatment, and it has been demonstrated that AA at 5 mg L^{-1} significantly inhibits root and shoot growth in lettuce seedlings [35]. Crucially, the observed rhizosphere effect accelerated PBAT–MP degradation and led to a significant enrichment of these byproducts directly in the root zone. This localized accumulation raises concerns regarding long-term ecological risks, particularly the potential for chronic phytotoxicity to hinder plant development and disrupt soil ecosystem health.

SEM images showed that large PBAT–MPs, initially smooth-surfaced, developed surface roughness and cavities after cultivation (Supplementary Fig. S10). In contrast, small PBAT–MPs had similar surface structural damage before and after cultivation. ATR–FTIR and Raman spectroscopy showed decreased functional group intensities in PBAT–MPs across sizes (Supplementary Figs. S11 and S12), indicating surface aging of the polymer [36]. The broad peak observed in the ATR–FTIR spectrum of the large PBAT–MPs after cultivation, spanning 3100–3500 cm^{-1}, indicates the formation of –OH groups resulting from ester bond cleavage [37].

NMR analysis further confirmed an elevated terephthalate-to-adipate ratio of PBAT–MPs after cultivation (Fig. 1e) [2]. Specifically, this ratio increased by 0.8% and 5.5% for large PBAT–MPs and by 3.9% and 3.0% for small PBAT–MPs in bulk and rhizosphere soils, respectively (Fig. 1e and Supplementary Fig. S13). The elevated terephthalate-to-adipate ratio aligns with preferential adipate unit degradation and the substantial AA accumulation observed (Fig. 1d). The TGA analysis showed a more pronounced high-temperature shift in the TG curves of both small and large PBAT–MPs in rhizosphere soil compared to the bulk soil (Supplementary Fig. S14a). DSC analysis revealed increased melting temperatures with large PBAT–MPs increasing from 125.0 to 127.9 and 130.2 °C in the bulk and rhizosphere soil, respectively. Meanwhile, small PBAT–MPs increased from 123.6 to 126.3 and 129.8 °C in the bulk and rhizosphere soil, respectively (Supplementary Fig. S14b). These changes in thermal properties further suggest a reduction in the molecular weights of PBAT–MPs [38].

Although these observations showed more advanced degradation in the rhizosphere soil, the overall structural integrity remained comparable to that of the original PBAT–MPs. Collectively, these findings support a surface-erosion mechanism of PBAT degradation, in which enzymatic removal of surface layers occurs while the underlying polymer matrix retains its structural integrity [39].

3.2. Role of soil aggregation in PBAT–MP degradation

Soybean cultivation typically enhances soil aggregation [40], and we observed a similar pattern in this study. Compared with the bulk soil, the proportions of the silt and clay fractions in the rhizosphere soil significantly decreased by 12.3%, 9.1%, and 13.9% in the BLK, L0.1, and L1 treatment groups, respectively ($p < 0.05$; Fig. 2). Conversely, the proportion of macroaggregates significantly increased in the BLK, L1, S0.1, and S1 treatments by 57.1%, 23.1%, 33.5%, and 62.8%, respectively ($p < 0.05$; Fig. 2). A notable 75.8% increase in mega-aggregates was also observed under the L1 treatment ($p < 0.05$; Fig. 2). Although improved soil aggregation enhances aeration and microbial activity [41], potentially aiding PBAT–MP degradation, significant degradation was detected only for large PBAT–MPs at high concentrations in rhizosphere soil (Fig. 1a).

We propose that PBAT–MP degradation is regulated by both particle size and concentration via interactions with soil aggregation. Previous studies have shown that small particulate MPs predominantly resided within microaggregates, whereas larger, film- or fragment-shaped particles were primarily associated with macroaggregates or remained unbound [42,43]. In this current study, soil aggregates physically sequestered small PBAT–MPs, potentially limiting their exposure to degradative enzymes. By contrast, larger PBAT–MPs exhibited reduced incorporation into aggregates, resulting in greater surface exposure within soil pores and enhanced enzyme accessibility despite their lower specific surface area. The 1% large PBAT–MPs improved soil aggregation (Fig. 2), thereby contributing to their significant degradation in rhizosphere soil (Fig. 1a).

However, the “accelerated degradation” observed at high PBAT–MP concentrations may not occur under environmentally relevant levels, as evidenced by the lack of significant degradation in the 0.1% large PBAT–MP treatment. In natural agricultural ecosystems, PBAT–MP inputs are typically low and spatially dispersed, reducing their potential to promote large aggregate formation and likely resulting in slower biodegradation rates. Therefore, future research should focus on the long-term behavior and ecological safety of PBAT–MPs at environmentally relevant concentrations.

3.3. The rhizosphere as a biogeochemical hotspot driving PBAT–MP degradation

Changes in soil properties were primarily driven by soybean cultivation. The soil pH values in the BLK, L1, and S1 treatments were significantly increased from 4.83, 4.79, and 4.76 to 4.96, 4.99, and 4.93, respectively ($p < 0.05$; Fig. 3a). DOC in rhizosphere soil of the BLK, L0.1, L1, S0.1, and S1 treatments increased significantly by 10.6%, 17.3%, 13.6%, 8.0%, and 10.9%, respectively, compared to the bulk soil ($p < 0.05$; Fig. 3b). MBC in the L0.1, L1, and S1 treatments increased significantly by 88.9%, 67.9%, and 17.1%, respectively, relative to the bulk soil ($p < 0.05$; Fig. 3c).

Nitrogen contents (DON, NH_4^+-N, and NO_3^--N) in the rhizosphere soil across all treatments were significantly lower than those in the bulk soil ($p < 0.05$; Fig. 3d–f). These shifts occurred because soybean roots release metabolites—sugars, organic acids, and amino acids—that stimulate microbial proliferation and enhance the decomposition of soil organic matter [7,44]. Additionally, soybean roots accelerate organic nitrogen mineralization, facilitating inorganic nitrogen uptake by plants and microorganisms [45,46]. This process is often accompanied by an unequal uptake of anions and cations. When anion uptake (particularly nitrate) exceeds cation uptake, plant roots release hydroxide or bicarbonate ions to maintain electrochemical balance, thereby elevating the rhizosphere pH above that of the bulk soil [47].

In this current study, the changes in soil properties driven by soybean cultivation created a complex environment for the degradation of PBAT–MPs. The observed increases in rhizosphere pH, DOC, and MBC established conditions that were generally favorable for PBAT–MP degradation. Specifically, elevated soil pH can indirectly promote PBAT degradation by increasing the activity of hydrolytic enzymes [10]. The higher microbial biomass stimulated by root exudates suggests a greater potential for microbially

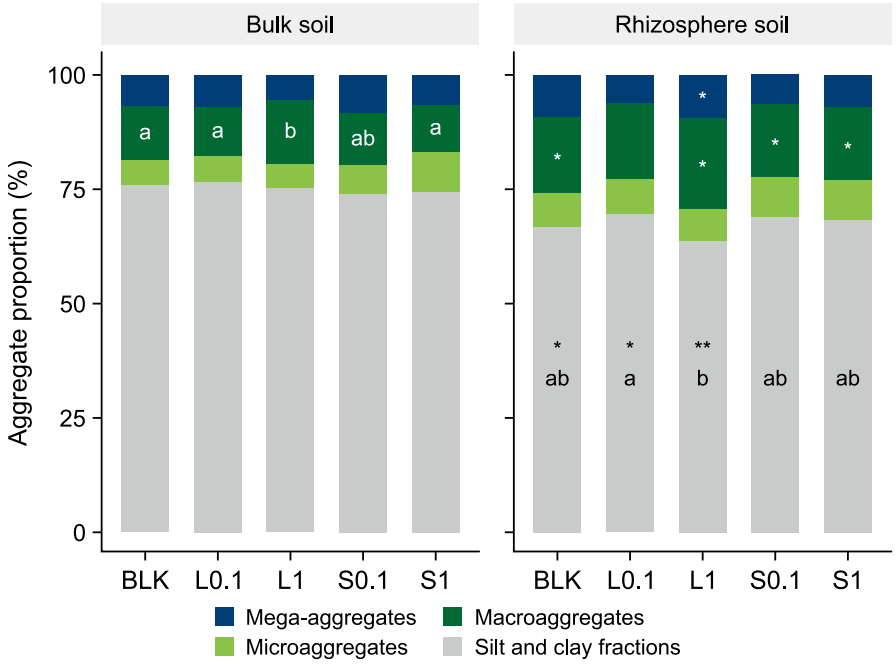

Fig. 2. Water-stable aggregate composition in bulk and rhizosphere soil. Lowercase letters indicate significant differences among treatments within each compartment ($p < 0.05$); asterisks indicate bulk vs. rhizosphere differences (*$p < 0.05$; **$p < 0.01$). BLK: no poly(butylene adipate-co-terephthalate) microplastics (PBAT–MPs) amended; L0.1 and L1: 0.1% and 1% large PBAT–MPs; S0.1 and S1: 0.1% and 1% small PBAT–MPs.

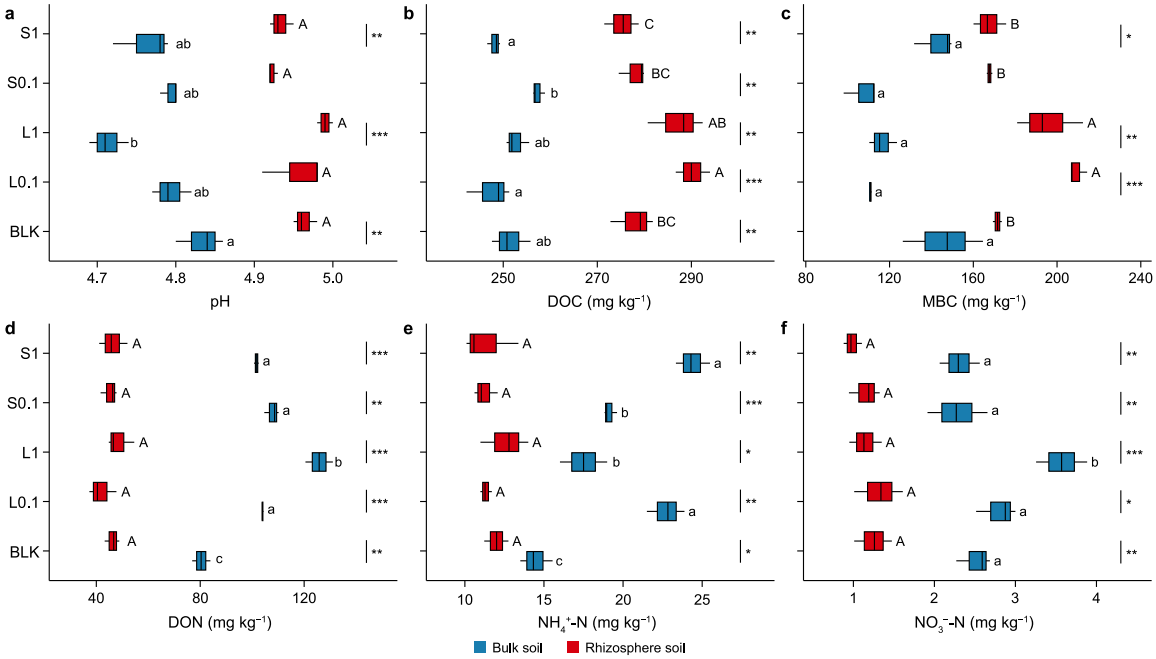

Fig. 3. Soil physicochemical properties in bulk and rhizosphere soils after soybean maturation. pH (**a**), dissolved organic carbon (DOC; **b**), microbial biomass carbon (MBC; **c**), dissolved organic nitrogen (DON; **d**), ammonium nitrogen (NH_4^+-N; **e**), and nitrate nitrogen (NO_3^--N; **f**). The central vertical lines represent the median, box limits indicate the 25th and 75th percentiles, and whiskers extend to the minimum and maximum values. Lowercase and uppercase letters indicate differences among treatments in bulk and rhizosphere soils, respectively ($p < 0.05$); asterisks indicate bulk vs. rhizosphere differences (*$p < 0.05$; **$p < 0.01$; ***$p < 0.001$). BLK: no poly(butylene adipate-co-terephthalate) microplastics (PBAT–MPs) amended; L0.1 and L1: 0.1% and 1% large PBAT–MPs; S0.1 and S1: 0.1% and 1% small PBAT–MPs.

driven degradation processes in the rhizosphere [48]. However, these favorable conditions were offset by a significant decrease in nitrogen content in the rhizosphere soil.

The depletion of available nitrogen is detrimental to PBAT–MP degradation because microorganisms require sufficient nitrogen for cell maintenance and the synthesis of enzymes necessary for polymer degradation [49]. Consequently, accelerated degradation of PBAT–MPs was observed exclusively in the L1 group. This

indicates that the net effect of the rhizosphere on PBAT–MP degradation is conditional on MPs' size and concentration. As demonstrated in Section 3.2, the 1% large PBAT–MPs improved soil aggregation, while the particles themselves were less incorporated into these aggregates. This increased their surface-area exposure and bioavailability to microbial attack. In contrast, the 0.1% large PBAT–MPs and both concentrations of small PBAT–MPs did not show significant degradation ($p > 0.05$), likely because their impact on the soil aggregate structure was less pronounced (Fig. 2a), thereby limiting their accessibility to microbial degradation.

PBAT–MPs exerted distinct effects on bulk and rhizosphere soil properties. Specifically, the pH and nitrogen content in the bulk soil were more susceptible to PBAT–MP influences (Fig. 3). In the L1 treatment, the bulk soil pH decreased significantly from 4.83 to 4.71 compared to the BLK ($p < 0.05$; Fig. 3a). The DON content in the bulk soil rose significantly by 29.4%, 56.5%, 34.1%, and 26.5% in the L0.1, L1, S0.1, and S1 treatments, respectively, compared to BLK ($p < 0.05$; Fig. 3d). Compared to BLK, NH_4^+-N content in the bulk soil significantly increased by 57.3%, 21.0%, 32.4%, and 68.6% in the L0.1, L1, S0.1, and S1 treatments, respectively ($p < 0.05$; Fig. 3e). Similarly, NO_3^--N content in the bulk soil of the L1 treatment increased significantly by 41.7% relative to BLK ($p < 0.05$; Fig. 3f).

Given that the PBAT–MPs themselves did not exhibit significant degradation in the bulk soil, these changes in soil properties are indirect. A plausible mechanism is that PBAT–MPs stimulate microorganisms to secrete more extracellular enzymes, thereby accelerating the decomposition of native soil organic matter through a positive priming effect [50]. This process releases substantial amounts of DON, an effect that was particularly evident in the L1 treatment. Due to increased DON availability, mineralization and subsequent nitrification rates were significantly enhanced, leading to elevated NH_4^+-N and NO_3^--N contents [51]. Consequently, the surge in nitrification in the L1 treatment caused soil acidification by generating H^+ ions [52], resulting in a decrease in soil pH.

In rhizosphere soil, DOC and MBC increased more in response to large PBAT–MPs. The DOC in the rhizosphere soil of the L0.1 treatment increased significantly, by 4.4%, compared to BLK ($p < 0.05$; Fig. 3b). The MBC in rhizosphere soil of the L0.1 and L1 treatments significantly increased by 22.1% and 14.0%, respectively, relative to BLK ($p < 0.05$; Fig. 3c). Previous studies have also found that 0.2–1.0% PBAT–MPs increase DOC and MBC contents in soybean rhizosphere soils, possibly because PBAT–MPs act as carbon sources for soil microorganisms, thereby stimulating microbial activity [53].

The FI, BIX, and HIX are indicators that describe the origin, autotrophic productivity, and humification of DOM, respectively [54]. The FI values exceeding 1.7 across all samples and the stable BIX index under varying treatments (Supplementary Fig. S15a and b) indicate that DOM in our soil predominantly originates from microbial activity, with microbially derived organics remaining unaffected by PBAT–MPs [29]. However, the HIX values for DOM from the rhizosphere soil were significantly lower than those from the bulk soil in the BLK, L0.1, and L1 groups, with reductions of 22.9%, 22.7%, and 29.2%, respectively ($p < 0.01$; Supplementary Fig. S15c).

The low degree of DOM humification suggests that the rhizosphere soil is enriched with copiotrophic species, which rapidly decompose low-molecular-weight carbon compounds to support their growth, in contrast to species that decompose complex organic compounds more slowly [55]. The addition of PBAT–MPs tended to reduce soil HIX values. Specifically, 0.1% small PBAT–MPs significantly reduced HIX in rhizosphere soil by 8.9%, while 1% small PBAT–MPs significantly lowered HIX in the bulk soil by 13.4% ($p < 0.05$; Supplementary Fig. S15c). While degradation products of PBAT–MPs have been shown to increase soil DOM humification [56], we observed a decrease in HIX values without significant PBAT–MP degradation. This suggests that PBAT–MPs altered the soil microenvironment, favoring a microbial community that produces less humified, protein-like DOM [57].

The parallel factor analysis model identified six components (Supplementary Fig. S16) from the EEM database of all samples, as detailed in Supplementary Table S3. C1 was excluded from subsequent analysis due to its probable classification as a fluorometer artifact. C2, C3, C4, and C5 represent humic-like substances, while C6 is a tryptophan-like component. The five remaining components, excluding C1, exhibited higher loadings for DOM from rhizosphere soil than from bulk soil, indicating active microbial secretions and root-driven inputs [58]. Additionally, PBAT–MPs did not significantly alter the proportional distribution of these five components in DOM from either the bulk soil or the rhizosphere soil (Supplementary Fig. S15d). This suggests that PBAT–MPs indirectly regulate DOM quality by inducing shifts in the microbial community rather than directly altering DOM composition [57], a finding consistent with the observed HIX trends. Approximately half of the enzymes known to degrade PBAT are esterases, and their activity in soil is associated with PBAT degradation [31,59]. However, soil esterase activity showed significant differences only in the S0.1 treatment, with rhizosphere soil exhibiting a 102.7% higher activity than bulk soil ($p < 0.01$; Supplementary Fig. S17). Notably, esterase activity on PBAT–MPs was 2.0- and 3.7-fold higher than the corresponding soil levels in bulk and rhizosphere soils, respectively (Fig. 4). This suggests that PBAT–MP surfaces develop a specialized plastisphere with enriched PBAT-degrading microbiota and depolymerases [12]. This enrichment is further pronounced in rhizosphere soil compared to bulk soil (Fig. 4).

3.4. Bacterial community structure and metabolic pathways driving PBAT–MP degradation in soil

Our findings indicate that the soil bacterial community responds to high concentrations of PBAT–MPs (1%) through community-level redundancy characterized by a high degree of structural resilience. NMDS analysis revealed that the rhizosphere and bulk soils had similar bacterial community structures at the mature stage of soybean growth, with no significant alterations induced by high concentrations of PBAT–MPs (1%) (Fig. 5a). Furthermore, neither the richness (ACE index) nor diversity (Shannon index) of bacterial communities at the ASV level differed significantly across treatment groups (Student's *t*-test, $p > 0.05$; Fig. 5b and Supplementary Fig. S18), underscoring the overall stability of the community. However, beneath this structural stability, we observed subtle reorganizations. The bacterial communities in the bulk and rhizosphere soils exhibited differential responses to PBAT–MP exposure, with more pronounced perturbations observed in the bulk soil. Notably, PBAT–MP exposure resulted in a higher proportion of unique ASVs in the bulk soil (B_L1: 38.1%, B_S1: 39.5%) compared to the rhizosphere soil (R_L1: 33.7%, R_S1: 29.2%) (Fig. 5c).

Over 90% of the bacterial taxa across all treatments belonged to six phyla (Chloroflexi, Proteobacteria, Actinobacteriota, Acidobacteriota, WPS-2, and Gemmatimonadota) (Fig. 5d). PBAT–MPs did not significantly alter the relative abundances of these phyla, except for a 40.9% reduction in the Actinobacteriota abundance in the B_S1 group compared to that in B_BLK ($p < 0.05$; Fig. 5d). Concurrently, the bacterial co-occurrence networks were restructured. All PBAT–MP treatments (1%) reduced the average degree of bacterial co-occurrence networks in the bulk

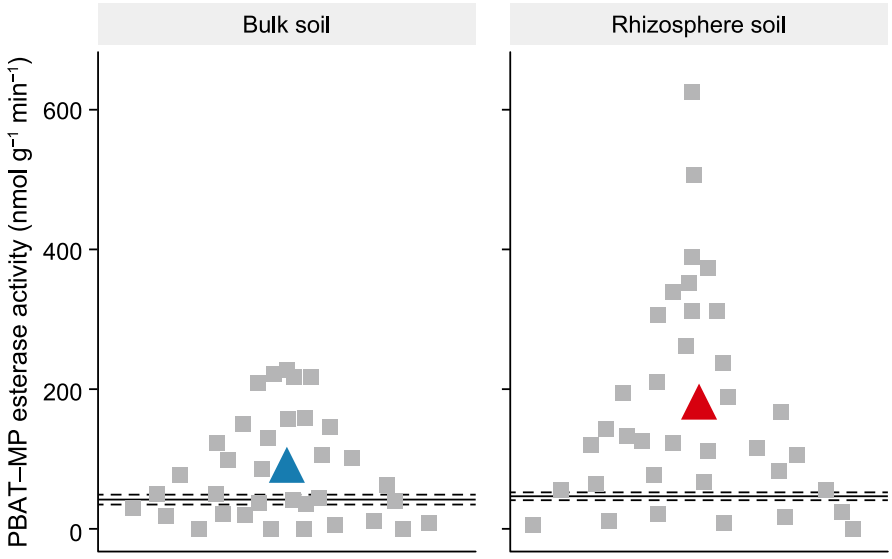

Fig. 4. Esterase activity on poly(butylene adipate-co-terephthalate) microplastic (PBAT–MP) particle surfaces. Gray square points are individual particle measurements, horizontally jittered to visualize the data distribution; triangles are compartment means. Solid and dashed black lines show the mean ± standard deviation of soil esterase activity. PBAT–MP esterase activity was significantly higher in rhizosphere soil than in bulk soil ($p < 0.01$).

(B_L1: −10.7%; B_S1: −14.7%) and rhizosphere soils (R_L1: −10.0%; R_S1: −4.0%), while positive correlations increased in most treatments (B_L1: +13.1%; B_S1: +11.7%; R_L1: +22.8%), except in R_S1 (−6.2%) (Fig. 5e).

The subtle shifts in the bacterial communities were directly linked to PBAT–MP degradation. Mantel tests identified significant associations between bacterial communities and soil properties, including PBAT residual rates ($p < 0.05$; Fig. 5f). Proteobacteria abundance correlated strongly with PBAT residuals ($p < 0.01$) and other soil parameters (SEA, pH, DOC, HIX, NO_3^--N, and DON; $p < 0.05$). Proteobacteria are the most abundant phylum producing carbohydrate-active enzymes and plastic-degrading enzymes (including various esterases) in the plastisphere of PBAT–MPs [60], playing a crucial role in PBAT degradation in soil [3,10].

Building on Han et al.'s [10] study, we analyzed changes in potential PBAT-degrading genera. Four potential PBAT-degrading genera—*Bradyrhizobium*, *Ramlibacter*, *Phenylobacterium*, and *Caulobacter*—all belong to the phylum Proteobacteria. However, only *Bradyrhizobium* and *Ramlibacter* showed significant enrichment in response to the presence of PBAT–MPs (Fig. 5g), indicating that these two genera were the primary degraders in the studied soils. *Bradyrhizobium* likely exploits its hydrolytic enzymes—originally evolved for plant–microbe interactions—to target PBAT ester bonds [61]. This capability stems from a genomic cluster encoding key enzymes, including endoglucanases *gunA* and *gunA2*, pectin methylesterase *pme*, and polygalacturonase *pgl*, which enable the breakdown of complex biopolymers and can be repurposed for synthetic substrates such as PBAT [62].

A recent metagenomic investigation identified the *tphB* gene in *Ramlibacter*, which encodes an enzyme essential for TPA metabolism, underscoring its potential for degrading terephthalate-based polyesters [63]. However, fungi are also crucial players in soils with strong enzymatic capacities to degrade complex polymers [64]. For instance, *Purpureocillium lilacinum* strain BA1S and *Aspergillus pseudodeflectus* isolated from farmland soils can degrade PBAT [65,66], and isotope labeling studies confirm that filamentous fungi assimilate carbon from PBAT monomers for energy and biomass [2]. Compared with the bulk soil, plant roots strongly reshaped fungal communities by providing labile carbon sources and releasing signaling molecules that recruited beneficial fungi [7,67]. Among them, arbuscular mycorrhizal fungi (AMF) are especially important because they form symbioses with most terrestrial plants, exchanging photosynthates for improved nutrient and water uptake [68]. Although no direct evidence indicates that AMF secrete enzymes to degrade PBAT, their extensive hyphal networks, soil aggregation, and reshaping of rhizosphere habitats [69]. These root-associated fungal effects may indirectly influence PBAT degradation, yet the underlying mechanisms require further investigation.

A total of 562 metabolites were detected in the bulk and rhizosphere soils. PLS–DA analysis demonstrated distinct metabolite profiles between the bulk soil and the rhizosphere soil, with clear separation along component 1 (35% variance) and component 2 (29% variance) (Fig. 6a). Notably, metabolite profiles in bulk soils underwent greater shifts than those in rhizosphere soils, as evidenced by the clustering of B_L1 and B_S1 farther away from their respective controls (B_BLK and R_BLK) (Fig. 6a). This pattern echoes the findings of Wang et al. [8], who observed stronger community and metabolic responses to MPs in unplanted soils, suggesting that the absence of root exudates creates an ecological vacancy that drives microbial niche specialization.

The addition of PBAT–MPs mainly caused significant changes in metabolites, such as lipids and lipid-like molecules, organic oxygen compounds, organoheterocyclic compounds, organic acids and derivatives, and benzenoids (Fig. 6b). In the bulk soil, large PBAT–MPs (1% w/w) upregulated all differential metabolites within the benzenoids and organohalogen compound categories (100% upregulation), while most other metabolic categories were downregulated. In contrast, small PBAT–MPs (1% w/w) upregulated 71.4% of differential metabolites in lipids and lipid-like molecules, 75.0% in organic acids and derivatives, and 75.0% in phenylpropanoids and polyketides, with the remaining categories mostly downregulated. In the rhizosphere soil, large PBAT–MPs upregulated 100% of differential metabolites in organic oxygen compounds and benzenoids, along with 66.7% in organic acids and derivatives, while small PBAT–MPs elevated 63.6% of differential metabolites in lipids and lipid-like molecules, 75% in organic acids and derivatives, and all (100%) in organosulfur compounds, with

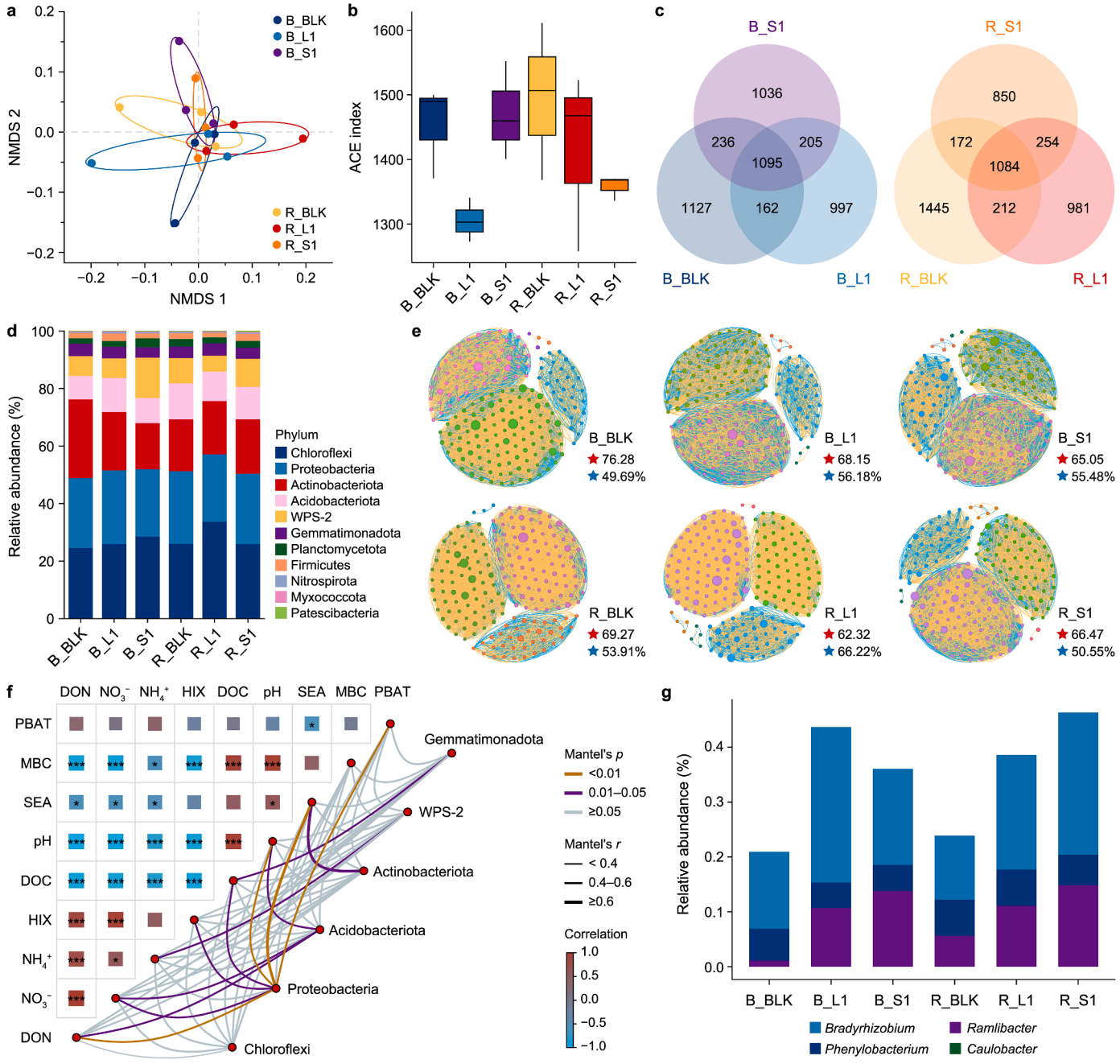

Fig. 5. Response of the soil bacterial community to poly(butylene adipate-co-terephthalate) microplastic (PBAT–MP) amendment. **a**, Nonmetric multidimensional scaling (NMDS) analysis of the bacterial community compositions based on Bray–Curtis similarities. Ellipses represent the 95% confidence intervals for each treatment group. **b**, Abundance-based coverage estimator (ACE) index of the bacterial community at the amplicon sequence variant (ASV) level. The central horizontal lines represent the median, box limits indicate the 25th and 75th percentiles, and whiskers extend to the minimum and maximum values. **c**, Venn diagram of bacterial communities at the ASV level. **d**, Relative abundance of bacterial community composition components at the phylum level. **e**, Co-occurrence network of bacterial communities (Spearman $\rho > 0.6$, $p < 0.05$). Edge colors indicate positive (yellow) and negative (blue) associations; node size scales with ASV relative abundance. Red star: average degree; blue star: positive correlation. **f**, Mantel test analysis of the relationship between bacterial communities and environmental factors. Significance is shown as $^{*}p < 0.05$; $^{**}p < 0.01$; $^{***}p < 0.001$. **g**, Relative abundance of potential PBAT-degrading genera. B_BLK and R_BLK: bulk and rhizosphere soils without PBAT–MPs amendment; B_L1 and R_L1: soils amended with 1% large PBAT–MPs; B_S1 and R_S1: soils amended with 1% small PBAT–MPs.

other categories predominantly downregulated.

Furthermore, the content of these substances mostly showed a negative correlation with PBAT–MP degradation rates ($\rho > 0.6$, $p < 0.05$; Fig. 6c). The main hydrolysis products of PBAT fall within these categories (AA belongs to lipids and lipid-like molecules, 1,4-butanediol belongs to organic oxygen compounds, and TPA belongs to benzenoids), indicating that PBAT-degrading bacteria simultaneously mineralized similar substances while degrading PBAT and utilizing its degradation products. Xanthobacteraceae (including *Bradyrhizobium*) and Comamonadaceae (including *Ramlibacter*) were the two families significantly correlated with PBAT–MP degradation rates ($\rho > 0.6$, $p < 0.05$; Fig. 6c).

Xanthobacteraceae induced significant changes in benzenoids, lipids, and lipid-like molecules, while Comamonadaceae induced

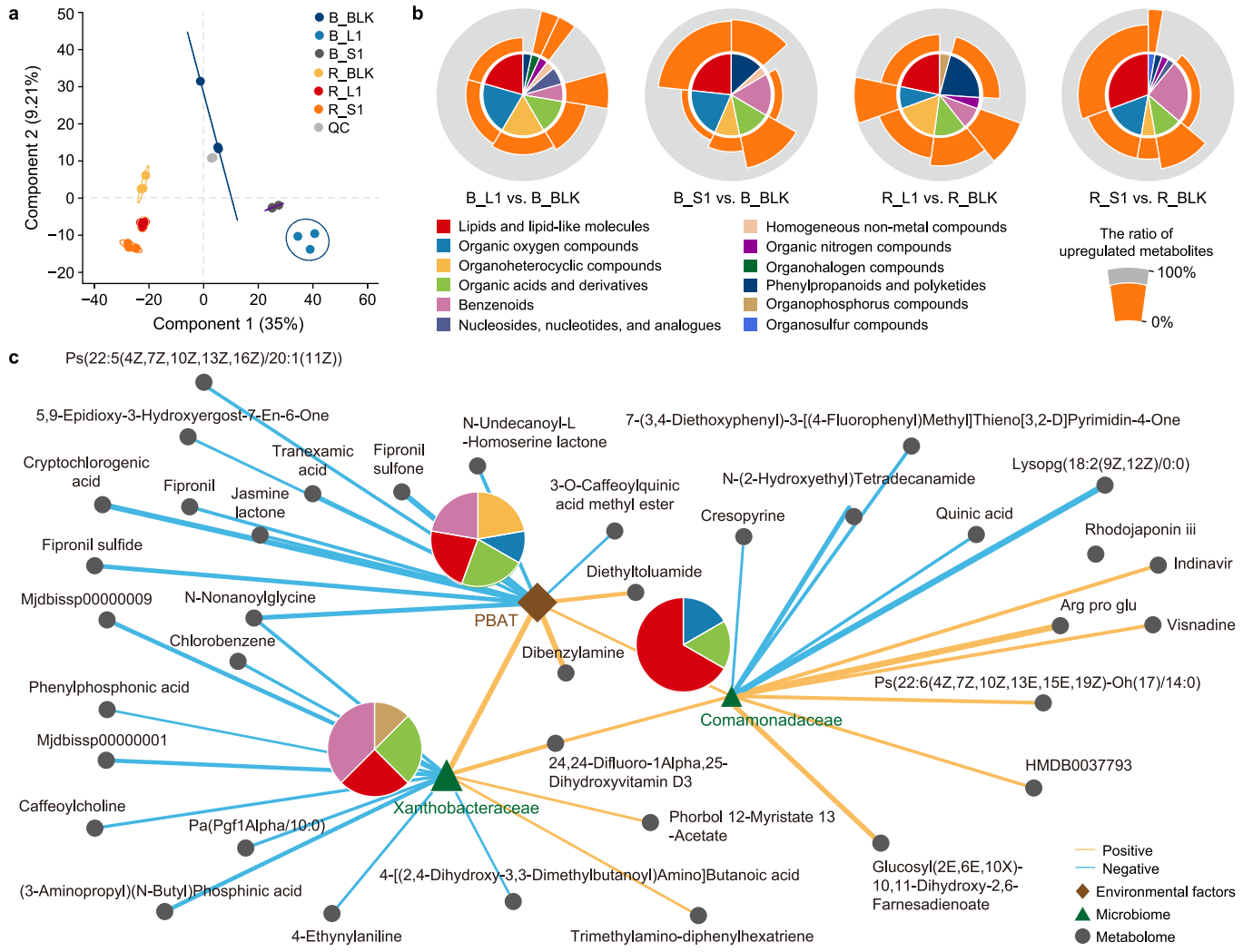

Fig. 6. Soil metabolome responses to poly(butylene adipate-co-terephthalate) microplastic (PBAT–MP) amendment. **a**, Partial least squares discriminant analysis (PLS–DA) score plots of soil metabolites. Ellipses represent the 95% confidence intervals for each treatment group. **b**, Distribution of differential metabolites identified from PLS–DA (variable importance in projection >1, $p < 0.05$). The pie chart illustrates the proportion of differential metabolites across categories, with the height of the orange sector indicating the proportion of upregulated metabolites in each category. **c**, Co-occurrence network of the degradation rate of PBAT–MPs, bacterial families, and soil metabolites (Spearman $\rho > 0.6$, $p < 0.05$. Edge colors indicate positive (yellow) and negative (blue) associations; edge thickness reflects correlation strength. Green triangular nodes correspond to the abundance of bacterial families. Pie charts display the distribution of metabolite types that are significantly correlated with the PBAT–MP degradation rate and with bacterial families, respectively. B_BLK and R_BLK: bulk and rhizosphere soils without PBAT–MPs amendment; B_L1 and R_L1: soils amended with 1% large PBAT–MPs; B_S1 and R_S1: soils amended with 1% small PBAT–MPs.

significant changes in organic oxygen compounds and lipids and lipid-like molecules. This suggests that bacteria from Xanthobacteraceae and Comamonadaceae have different metabolic modes for degrading PBAT–MPs. Although both can secrete esterases and metabolize AA, bacteria in Xanthobacteraceae may mainly metabolize terephthalic acid, while those in Comamonadaceae may mainly metabolize 1,4-butanediol. This differential metabolic preference highlights the complex interactions between microbial taxa and PBAT–MP degradation pathways in soil environments.

3.5. Mechanism for the degradation of PBAT–MPs in agricultural soil

Based on our experimental evidence, we propose a three-part mechanistic framework for PBAT–MP degradation in agricultural soils. First, the incorporation status of PBAT–MPs within soil aggregates governs their bioaccessibility, with reduced sequestration enhancing degradability. In our study, large PBAT–MPs exhibited limited incorporation into aggregates, positioning them within soil pores where they remained more exposed and bioavailable for microbial attack.

Second, the rhizosphere functions as a conditional hotspot whose net effect—whether promoting or inhibiting degradation—depends on a complex balance of competing factors. Although elevated pH and microbial activity in our rhizosphere soil overcame nitrogen limitations, enabling the significant degradation of large PBAT–MPs, this phenomenon may not be universally observable. Under typical conditions, rhizosphere pH is lower than that of bulk soil, which can inhibit depolymerase activity [10]. Thus, the rhizosphere effect is contingent on specific combinations of particle size, concentration, and soil properties.

Third, PBAT–MP degradation proceeds via the microbial colonization of particle surfaces and the secretion of specialized

depolymerases [2]. This process is driven by preferential hydrolysis of aliphatic adipate units, which initiates surface erosion, while the underlying polymer matrix retains structural integrity. Degradation generates intermediate oligomers and three monomeric products [24,70], the microbial utilization of which concurrently modulates the metabolism of analogous soil substances (e.g., lipids and benzenoids).

4. Conclusion

This study demonstrated that the rhizosphere's capacity to enhance PBAT–MP degradation is highly conditional, depending on specific combinations of particle size, concentration, and soil conditions rather than acting as a universal accelerator. A critical finding is that accelerated degradation can simultaneously enrich phytotoxic monomers directly within a root zone, challenging the assumption that root-mediated biodegradation is inherently ecobeneficial.

Our short-term pot experiment focused on bacterial communities and used homogenized soil, which limited our ability to capture natural rhizosphere heterogeneity. As a result, it offers only a constrained view of long-term field dynamics, where fungi and multiseasonal accumulation can be important. Notably, although we quantified monomer accumulation, direct mineralization data for these products and intermediate oligomers are lacking. Future studies should prioritize multiyear field trials to trace the complete fate of polymers, including nanoplastic formation, across diverse crops and soil types. Integrated microbiome analyses encompassing bacteria and fungi, coupled with isotopic tracing to quantify mineralization and spatially resolved sampling, are essential for elucidating complete carbon pathways and identifying functional degraders under realistic rhizosphere conditions.

Biodegradable mulches should not be assumed to self-degrade in soil. Current application practices may lead to persistent BMP accumulation, particularly for smaller particles that become physically protected within aggregates. Management strategies must include establishing soil-monitoring protocols for monomer and oligomer accumulation near root zones and reforming biodegradability certifications to require rhizosphere-relevant testing with pass/fail criteria for the generation of toxic byproducts. Without such measures, biodegradable plastics risk becoming a source of chronic contamination rather than a sustainable solution to agricultural plastic pollution.

CRediT authorship contribution statement

Kailin Gong: Writing – original draft, Methodology, Investigation, Data curation, Conceptualization, Formal analysis, Software, Validation, Visualization. **Cheng Peng:** Writing – review & editing, Supervision, Resources, Project administration, Conceptualization, Funding acquisition, Methodology. **Xiaoyi Chen:** Investigation. **Li Cai:** Writing – review & editing. **Wei Zhang:** Writing – review & editing, Resources.

Data availability

The raw sequencing data have been deposited in National Center for Biotechnology Information under accession number PRJNA1237425, and the metabolomics data have been deposited in MetaboLights under accession number MTBLS12524. Other data used in this study are available upon reasonable request.

Declaration of competing interest

The authors declare that they have no known competing financial interests or personal relationships that could have appeared to influence the work reported in this paper.

Acknowledgements

This work was supported by the National Key Research and Development Program of China (2023YFC3711600) and the National Natural Science Foundation of China (42577465 and 42177395). We thank the staff at the BL01B beamline of the National Facility for Protein Science in Shanghai, Shanghai Advanced Research Institute, Chinese Academy of Sciences, for providing technical support and assistance with data collection and analysis. The authors thank the Research Center for Analysis and Testing at East China University of Science and Technology for their assistance with the analysis and testing. The authors extend their gratitude to Ms. Tingting Wang from Shiyanjia Lab (www.shiyanjia.com) for providing invaluable assistance with the SEM analysis.

Appendix A. Supplementary data

Supplementary data to this article can be found online at https://doi.org/10.1016/j.ese.2026.100678.

References

[1] X. Hu, H. Gu, X. Sun, Y. Wang, J. Liu, Z. Yu, Y. Li, J. Jin, G. Wang, Distinct influence of conventional and biodegradable microplastics on microbe-driving nitrogen cycling processes in soils and plastispheres as evaluated by metagenomic analysis, J. Hazard. Mater. 451 (2023) 131097.
[2] M.T. Zumstein, A. Schintlmeister, T.F. Nelson, R. Baumgartner, D. Woebken, M. Wagner, H.-P.E. Kohler, K. McNeill, M. Sander, Biodegradation of synthetic polymers in soils: tracking carbon into CO_2 and microbial biomass, Sci. Adv. 4 (2018) eaas9024.
[3] M. Chen, M. Cao, W. Zhang, X. Chen, H. Liu, Z. Ning, L. Peng, C. Fan, D. Wu, M. Zhang, Q. Li, Effect of biodegradable PBAT microplastics on the C and N accumulation of functional organic pools in tropical latosol, Environ. Int. 183 (2024) 108393.
[4] P. Fan, H. Yu, B. Xi, W. Tan, A review on the occurrence and influence of biodegradable microplastics in soil ecosystems: are biodegradable plastics substitute or threat? Environ. Int. 163 (2022) 107244.
[5] Y. Huo, F.A. Dijkstra, M. Possell, B. Singh, Mineralisation and priming effects of a biodegradable plastic mulch film in soils: influence of soil type, temperature and plastic particle size, Soil Biol. Biochem. 189 (2024) 109257.
[6] L. Schöpfer, U. Schnepf, S. Marhan, F. Brümmer, E. Kandeler, H. Pagel, Hydrolyzable microplastics in soil—low biodegradation but formation of a specific microbial habitat? Biol. Fertil. Soils 58 (2022) 471–486.
[7] A. Sugiyama, The soybean rhizosphere: metabolites, microbes, and beyond—A review, J. Adv. Res. 19 (2019) 67–73.
[8] Q. Wang, W. Liu, Q. Zhou, S. Wang, F. Mo, X. Wu, J. Wang, R. Shi, X. Li, C. Yin, Y. Sun, Planting enhances soil resistance to microplastics: evidence from carbon emissions and dissolved organic matter stability, Environ. Sci. Technol. 58 (2024) 21327–21338.
[9] X. Ma, M. Zarebanadkouki, Y. Kuzyakov, E. Blagodatskaya, J. Pausch, B.S. Razavi, Spatial patterns of enzyme activities in the rhizosphere: effects of root hairs and root radius, Soil Biol. Biochem. 118 (2018) 69–78.
[10] Y. Han, Y. Teng, X. Wang, W. Ren, X. Wang, Y. Luo, H. Zhang, P. Christie, Soil type driven change in microbial community affects poly(butylene adipate-co-terephthalate) degradation potential, Environ. Sci. Technol. 55 (2021) 4648–4657.
[11] L.M. York, A. Carminati, S.J. Mooney, K. Ritz, M.J. Bennett, The holistic rhizosphere: integrating zones, processes, and semantics in the soil influenced by roots, J. Exp. Bot. 67 (2016) 3629–3643.
[12] M.C. Rillig, S.W. Kim, Y.-G. Zhu, The soil plastisphere, Nat. Rev. Microbiol. 22 (2024) 64–74.
[13] N. Ling, T. Wang, Y. Kuzyakov, Rhizosphere bacteriome structure and functions, Nat. Commun. 13 (2022) 836.
[14] Y. Zhang, J. Ma, Y.-Q. Song, G. Li, P. O'Connor, Stronger deterministic processes shape the plastisphere microbiota of biodegradable microplastics compared to non-biodegradable microplastics in farmland soil, Appl. Soil Ecol. 196 (2024) 105312.
[15] Y. Han, Y. Teng, X. Wang, D. Wen, P. Gao, D. Yan, N. Yang, Biodegradable PBAT microplastics adversely affect pakchoi (*Brassica chinensis* L.) growth and the

rhizosphere ecology: focusing on rhizosphere microbial community composition, element metabolic potential, and root exudates, Sci. Total Environ. 912 (2024) 169048.
[16] X. Li, X. Cheng, J. Wu, Z. Cai, Z. Wang, J. Zhou, Multi-omics reveals different impact patterns of conventional and biodegradable microplastics on the crop rhizosphere in a biofertilizer environment, J. Hazard. Mater. 467 (2024) 133709.
[17] Y. Wang, Z. Zhao, M. Jiao, T. Li, Y. Wei, R. Li, G. Peng, Rhizospheric bacterial communities against microplastics (MPs): novel ecological strategies based on the niche differentiation, J. Hazard. Mater. 480 (2024) 135806.
[18] K. Janczak, K. Hrynkiewicz, Z. Znajewska, G. Dąbrowska, Use of rhizosphere microorganisms in the biodegradation of PLA and PET polymers in compost soil, Int. Biodeterior. Biodegrad. 130 (2018) 65–75.
[19] K. Janczak, G.B. Dąbrowska, A. Raszkowska-Kaczor, D. Kaczor, K. Hrynkiewicz, A. Richert, Biodegradation of the plastics PLA and PET in cultivated soil with the participation of microorganisms and plants, Int. Biodeterior. Biodegrad. 155 (2020) 105087.
[20] T.F. Nelson, R. Baumgartner, M. Jaggi, S.M. Bernasconi, G. Battagliarin, C. Sinkel, A. Kunkel, H.E. Kohler, K. McNeill, M. Sander, Biodegradation of poly(butylene succinate) in soil laboratory incubations assessed by stable carbon isotope labelling, Nat. Commun. 13 (2022) 5691.
[21] T.F. Nelson, S.C. Remke, H.-P.E. Kohler, K. McNeill, M. Sander, Quantification of synthetic polyesters from biodegradable mulch films in soils, Environ. Sci. Technol. 54 (2019) 266–275.
[22] M.S. Kim, H. Chang, L. Zheng, Q. Yan, B.F. Pfleger, J. Klier, K. Nelson, E.L.W. Majumder, G.W. Huber, A review of biodegradable plastics: chemistry, applications, properties, and future research needs, Chem. Rev. 123 (2023) 9915–9939.
[23] L. Nizzetto, G. Binda, R. Hurley, C. Baann, S. Selonen, S. Velmala, C.A.M. van Gestel, Comments to “Degli-Innocenti, F. The pathology of hype, hyperbole and publication bias is creating an unwarranted concern towards biodegradable mulch films” [J. Hazard. Mater. 463 (2024) 132923], J. Hazard. Mater. 471 (2024) 133690.
[24] Z. Hua, Y. Li, X. He, F. Zhu, S. Chang, J. Kong, C. Zhu, C. Wang, S. Li, H. He, C. Gu, Quantitative analysis of PBAT microplastics and their degradation products in soil by mass spectrometry, Eco-Environ. Health 4 (2025) 100166.
[25] S. Li, F. Ding, M. Flury, J. Wang, Dynamics of macroplastics and microplastics formed by biodegradable mulch film in an agricultural field, Sci. Total Environ. 894 (2023) 164674.
[26] T. Yamashita, H. Flessa, B. John, M. Helfrich, B. Ludwig, Organic matter in density fractions of water-stable aggregates in silty soils: effect of land use, Soil Biol. Biochem. 38 (2006) 3222–3234.
[27] E.D. Vance, P.C. Brookes, D.S. Jenkinson, An extraction method for measuring soil microbial biomass C, Soil Biol. Biochem. 19 (1987) 703–707.
[28] R. Lu, Methods in Soil Agricultural Chemical Analysis: I. Analysis of Chemical Properties of Soil and Water, China Agricultural Science and Technology Press, 1999.
[29] Y. Sun, X. Li, X. Li, J. Wang, Deciphering the fingerprint of dissolved organic matter in the soil amended with biodegradable and conventional microplastics based on optical and molecular signatures, Environ. Sci. Technol. 56 (2022) 15179–16540.
[30] N. Li, H. Du, M.-H. Li, R. Na, R. Dong, H.S. He, S. Zong, L. Huang, Z. Wu, Deyeuxia angustifolia upward migration and nitrogen deposition change soil microbial community structure in an alpine tundra, Soil Biol. Biochem. 180 (2023) 109009.
[31] S. Tsuboi, K. Yamamoto-Tamura, A. Takada, S. Yonemura, Y. Takada Hoshino, H. Kitamoto, A.W. Kishimoto-Mo, Selection of *p*-nitrophenyl fatty acid substrate suitable for detecting changes in soil esterase activity associated with degradation of biodegradable polyester mulch films: a field trial, Ital. J. Agron. 17 (2022).
[32] M. Siotto, E. Sezenna, S. Saponaro, F.D. Innocenti, M. Tosin, L. Bonomo, V. Mezzanotte, Kinetics of monomer biodegradation in soil, J. Environ. Manag. 93 (2012) 31–37.
[33] Q. Liu, X. zhang, J. Gao, S. Fan, W. Li, W. Li, W. Liu, J. Li, Q. Gu, Efficient and complete biodegradation of poly (butylene adipate-co-terephthalate) by a novel dual-member bacterial consortium from compost: Metabolic division of labor between BDP053 and BDT04, J. Hazard. Mater. 496 (2025) 139386.
[34] J. Ma, Y. Cao, L. Fan, Y. Xie, X. Zhou, Q. Ren, X. Yang, X. Gao, Y. Feng, Degradation characteristics of polybutylene adipate terephthalic acid (PBAT) and its effect on soil physicochemical properties: a comparative study with several polyethylene (PE) mulch films, J. Hazard. Mater. 456 (2023) 131661.
[35] L. Martin-Closas, R. Botet, A.M. Pelacho, An in vitro crop plant ecotoxicity test for agricultural bioplastic constituents, Polym. Degrad. Stabil. 108 (2014) 250–256.
[36] R. Tian, K. Li, Y. Lin, C. Lu, X. Duan, Characterization techniques of polymer aging: from beginning to end, Chem. Rev. 123 (2023) 3007–3088.
[37] K. Gutiérrez-Silva, A.J. Capezza, O. Gil-Castell, J.D. Badia-Valiente, UV-C and UV-C/H_2O-induced abiotic degradation of films of commercial PBAT/TPS blends, Polymers 17 (2025) 1173.
[38] Y.D. Hernandez-Charpak, H.J. Kansara, T.A. Trabold, J.S. Lodge, C.L. Lewis, C.A. Diaz, Application of differential scanning calorimetry to assess molecular weight degradation of poly(butylene adipate-co-terephthalate)-based plastics, ACS ES&T Eng. 5 (2025) 642–654.
[39] K. Meng, E.H. Lwanga, M. van der Zee, D.R. Munhoz, V. Geissen, Fragmentation and depolymerization of microplastics in the earthworm gut: a potential for microplastic bioremediation? J. Hazard. Mater. 447 (2023) 130765.
[40] M. Zhou, C. Liu, J. Wang, Q. Meng, Y. Yuan, X. Ma, X. Liu, Y. Zhu, G. Ding, J. Zhang, X. Zeng, W. Du, Soil aggregates stability and storage of soil organic carbon respond to cropping systems on black soils of Northeast China, Sci. Rep. 10 (2020) 265.
[41] C. Yang, N. Liu, Y. Zhang, Soil aggregates regulate the impact of soil bacterial and fungal communities on soil respiration, Geoderma 337 (2019) 444–452.
[42] Z. Wang, C. Chen, P. Su, Y. Xing, H. Zou, Y. Zhang, Abundance of microplastics in farmland soil and its distribution in soil aggregate fractions in the Liaoning area, J. Agro-Environ. Sci. 43 (2024) 858–865.
[43] Y. Liu, Y. Zhong, C. Hu, M. Xiao, F. Ding, Y. Yu, H. Yao, Z. Zhu, J. Chen, T. Ge, J. Ding, Distribution of microplastics in soil aggregates after film mulching, Soil Ecol. Lett. 5 (2023) 230171.
[44] M. Wang, A.-H. Ge, X. Ma, X. Wang, Q. Xie, L. Wang, X. Song, M. Jiang, W. Yang, J.D. Murray, Y. Wang, H. Liu, X. Cao, E. Wang, Dynamic root microbiome sustains soybean productivity under unbalanced fertilization, Nat. Commun. 15 (2024) 1668.
[45] Y. Liu, S.E. Evans, M.L. Friesen, L.K. Tiemann, Root exudates shift how N mineralization and N fixation contribute to the plant-available N supply in low fertility soils, Soil Biol. Biochem. 165 (2022) 108541.
[46] A.J. Miller, M.D. Cramer, Root nitrogen acquisition and assimilation, Plant Soil 274 (2005) 1–36.
[47] H. Li, L. Luo, B. Tang, H. Guo, Z. Cao, Q. Zeng, S. Chen, Z. Chen, Dynamic changes of rhizosphere soil bacterial community and nutrients in cadmium polluted soils with soybean-corn intercropping, BMC Microbiol. 22 (2022) 57.
[48] Q. Liao, H. Liu, C. Lu, J. Liu, M.G. Waigi, W. Ling, Root exudates enhance the PAH degradation and degrading gene abundance in soils, Sci. Total Environ. 764 (2021) 144436.
[49] L. Wang, Y. Qi, L. Cao, L. Song, R. Hu, Q. Li, Y. Zhao, J. Liu, H. Zhang, Promoting role of nitrogen-fixing bacteria and biochar on nitrogen retention and degradation of PBAT plastics during composting, Environ. Pollut. 363 (2024) 125228.
[50] S. Chang, C. Chen, Q.-L. Fu, A. Zhou, Z. Hua, F. Zhu, S. Li, H. He, PBAT biodegradable microplastics enhanced organic matter decomposition capacity and CO_2 emission in soils with and without straw residue, J. Hazard. Mater. 480 (2024) 135872.
[51] D.L. Jones, D. Shannon, D.V. Murphy, J. Farrar, Role of dissolved organic nitrogen (DON) in soil N cycling in grassland soils, Soil Biol. Biochem. 36 (2004) 749–756.
[52] P. Guan, R. Wang, J.N. Nkoh, R. Shi, X. Pan, J. Li, R. Xu, Enriching organic carbon bioavailability can mitigate soil acidification induced by nitrogen fertilization in croplands through microbial nitrogen immobilization, Soil Sci. Soc. Am. J. 86 (2022) 579–592.
[53] Y. Yu, Y. Wang, D.W.S. Tang, S. Xue, M. Liu, V. Geissen, X. Yang, Soil C-N and microbial community were altered by polybutylene adipate terephthalate microplastics, J. Hazard. Mater. 493 (2025) 138328.
[54] Y. Sun, J. Ji, J. Tao, Y. Yang, D. Wu, L. Han, S. Li, J. Wang, Current advances in interactions between microplastics and dissolved organic matters in aquatic and terrestrial ecosystems, Trac. Trends Anal. Chem. 158 (2023) 116882.
[55] I.V. Danilin, N.N. Danchenko, A.R. Ziganshina, Y.R. Farkhodov, N.V. Yaroslavtseva, V.A. Kholodov, Divergent response of chernozem organic matter towards short-term water stress in *Poa pratensis* L. rhizosphere and bulk soil in pot experiments: a spectroscopic study, Soil Tillage Res. 245 (2025) 106285.
[56] M. Chen, X. Zhao, D. Wu, L. Peng, C. Fan, W. Zhang, Q. Li, C. Ge, Addition of biodegradable microplastics alters the quantity and chemodiversity of dissolved organic matter in latosol, Sci. Total Environ. 816 (2022) 151960.
[57] L. Liu, L. Hu, Y. Kuzyakov, M.C. Rillig, G. Duan, G. Wei, C. Chen, Microbial physiological adaptation to biodegradable microplastics drives the transformation and reactivity of dissolved organic matter in soil, Environ. Sci. Technol. 59 (2025) 19856–19871.
[58] Y. Liu, Z. Hong, X. Huang, Y. Peng, J. Xu, Content of dissolved organic matter (DOM) and its fluorescence constitution in root areas of five mangrove plants in situ, Acta Sci. Circumstantiae 35 (2015) 2556–2562.
[59] V. Gambarini, O. Pantos, J.M. Kingsbury, L. Weaver, K.M. Handley, G. Lear, PlasticDB: a database of microorganisms and proteins linked to plastic biodegradation, Database 2022 (2022) baac008.
[60] X. Hu, H. Gu, X. Sun, Y. Wang, J. Liu, Z. Yu, Y. Li, J. Jin, G. Wang, Metagenomic exploration of microbial and enzymatic traits involved in microplastic biodegradation, Chemosphere 348 (2024) 140762.
[61] S. Vela, M.M. Häggblom, L.Y. Young, Biodegradation of aromatic and aliphatic compounds by rhizobial species, Soil Sci. 167 (2002) 802–810.
[62] I.C. Baumberger, N. Fraefel, M. Göttfert, H. Hennecke, New nodW- or nifA-regulated *Bradyrhizobium japonicum* genes, Mol. Plant Microbe Interact. 16 (2003) 342–351.
[63] Z. Hao, Q. Wang, Z. Yan, Y. Luo, H. Jiang, Hydrological fluctuations modulate potential plastic-degrading microbial communities in floodplains, ACS ES&T Wat 5 (2025) 6299–6309.
[64] E.J. Okal, G. Heng, E.A. Magige, S. Khan, S. Wu, Z. Ge, T. Zhang, P.E. Mortimer, J. Xu, Insights into the mechanisms involved in the fungal degradation of plastics, Ecotoxicol. Environ. Saf. 262 (2023) 115202.
[65] W.-S. Tseng, M.-J. Lee, J.-A. Wu, S.-L. Kuo, S.-L. Chang, S.-J. Huang, C.-T. Liu, Poly(butylene adipate-co-terephthalate) biodegradation by *Purpureocillium lilacinum* strain BA1S, Appl. Microbiol. Biotechnol. 107 (2023) 6057–6070.
[66] M. Fernandes, A.F. Salvador, A.A. Vicente, Biodegradation of PHB/PBAT films

and isolation of novel PBAT biodegraders from soil microbiomes, Chemosphere 362 (2024) 142696.
[67] V. Vives-Peris, C. de Ollas, A. Gómez-Cadenas, R.M. Pérez-Clemente, Root exudates: from plant to rhizosphere and beyond, Plant Cell Rep. 39 (2020) 3–17.
[68] M. Parniske, Arbuscular mycorrhiza: the mother of plant root endosymbioses, Nat. Rev. Microbiol. 6 (2008) 763–775.
[69] J. Zhang, R. Zhao, X. Li, J. Zhang, Potential of arbuscular mycorrhizal fungi for soil health: a review, Pedosphere 34 (2024) 279–288.
[70] Y. Wang, Q. Liu, C.-H. Xie, R.-T. Zhao, Q.-X. Tang, D.-F. Han, Y.-N. Xia, J.-X. Cui, C.-R. Yan, W.-Q. He, Bridging the knowledge gap: from poly(butylene adipate-co-terephthalatebutylene) degradation to CO_2-generating mineralization under the synergistic effect of bacteria and fungi, J. Hazard. Mater. 494 (2025) 138643.